

Supplementary Material for “The Occupied Electronic Structure of Ultrathin Boron Doped Diamond”

A. C. Pakpour-Tabrizi,¹ A. K. Schenk,² A. J. U. Holt,³ S. K. Mahatha,³
F. Arnold,³ M. Bianchi,³ R. B. Jackman,¹ J. E. Butler,⁴ A. Vikharev,⁵
J. A. Miwa,³ Ph. Hofmann,³ S. P. Cooil,^{2,6} J. W. Wells,^{2,*} and F. Mazzola^{2,†}

¹*London Centre for Nanotechnology and Department of
Electronic and Electrical Engineering, University College London,
17-19 Gordon Street, London WC1H 0AH, U.K.*

²*Center for Quantum Spintronics, Department of Physics,
Norwegian University of Science and Technology, NO-7491 Trondheim, Norway*

³*Department of Physics and Astronomy,
Interdisciplinary Nanoscience Center,
Aarhus University, 8000 Aarhus C, Denmark*

⁴*Cubic Carbon Ceramics, 855 Carson Road, Huntingtown, MD 20639, USA*

⁵*Institute of Applied Physics, Russian Academy of Sciences,
46 Ul'yanov Street , 603950, Nizhny Novgorod , Russia*

⁶*Department of Physics, Aberystwyth University,
Aberystwyth SY23 3BZ, United Kingdom*

(Dated: February 21, 2020)

* Corresponding author justin.wells@ntnu.no

† Present Address: SUPA, School of Physics and Astronomy, University of St. Andrews, St. Andrews, UK

I. EXPERIMENTAL DETAILS

The measurements described in this work use two boron-doped δ -layer samples with nominal thickness of 1.8 nm, and a thick (thickness $\sim 3 \mu\text{m}$) boron-doped thick film. The boron doped δ -layers was grown on a $3.6 \text{ mm} \times 3.6 \text{ mm}$ (100) oriented high pressure high temperature (HPHT) Ib substrate, with an intrinsic buffer layer (nominal thickness $0.5 \mu\text{m}$) grown using CVD between the δ -layer and substrate. One sample was grown at the Institute of Applied Physics, Russian Academy of Sciences (IAP RAS), and full details of the growth are in Ref. 1, and the second sample (grown similarly) was produced by Element Six Ltd., and full details of the growth may be found in Ref. 2.

The thick boron doped sample was grown with chemical vapour deposition (CVD). The boron doping density, determined with Secondary-Ion Mass Spectrometry (SIMS) is similar in both of these samples ($\sim 5 \times 10^{20} \text{ cm}^{-3}$). The boron doped thick film was grown using chemical vapour deposition (CVD) using a gas mixture of 60% trimethylborane ($\text{B}(\text{C}_2\text{H}_5)_3$), 5% methane (CH_4) and 35% hydrogen with a total pressure of 150 Torr. Growth was carried out in an Astex - AX6500 MEPCVD reactor for 120 minutes, with a microwave power of 1.9 kW and a substrate temperature of 1000°C . The boron doping density, determined with Secondary-Ion Mass Spectrometry (SIMS) is similar in all of these samples ($\sim 5 \times 10^{20} \text{ cm}^{-3}$).

The ARPES data presented here measured with photon energies above 190 eV was acquired at the VUV-Photoemission beamline (Elettra) and at the ADRESS beamline (SLS). Data below 190 eV was acquired on the I4 beamline at MAX-III. The *in situ* sample preparation, measurement conditions and data processing procedures are identical to those for the samples in the main text.

II. DEVIATION FROM THE FREE-ELECTRON FINAL STATE MODEL

As mentioned in the experimental details section of the main text, the ARPES measurements for this study have been performed at higher photon energies than are typical for ARPES. Low photon energies (below 50 eV) are generally preferred due to two experimental factors. Firstly, the photoionisation cross section for the orbitals contributing to the valence band, in the case of diamond the C2s and C2p orbitals, is up to three orders of magnitude larger for photon energies less than 50 eV when compared to those in the

range 50 – 460 eV.[3] Secondly, both energy and k_{\parallel} resolution tend to improve as the photon energy decreases,[4]. Given these factors, it is natural to question why the data presented in this article has been recorded at relatively high energy for ARPES. The reason is that the work of Himpsel *et al.* shows that diamond does not present free-electron final state (FEFS) behaviour for measurements acquired with photon energies below 100 eV [5]. Here we show that this is the case even at higher photon energy.

Fig. S2(a) shows a constant k_{\parallel} slice through data acquired on the bulk film sample with photon energies between 190 eV and 480 eV. It is expected that the bands will have a periodicity of 3.52 \AA^{-1} , given the diamond lattice constant of 3.57 \AA . However, between 190 eV and 280 eV it is not possible to make out any clear features (Fig S2(b) shows the data acquired at 220 eV), and the features present at 280 eV and 290 eV show no dispersion with k_{\parallel} , suggesting that they are the result of a second-harmonic excitation of the C1s core level. At even lower photon energy, structure returns. Data acquired at 30 eV and at 410 eV (Fig S1(a,b)), near the Brillouin zone center ($k_{\perp} = 10.76 \text{ \AA}^{-1}$, $3.69 \pm 0.15 \text{ \AA}^{-1}$), is in reasonable agreement with the results of tight binding (TB) calculations (shown in red). However, data acquired at 40 eV (Fig S1(c), $k_{\perp} = 4.03 \pm 0.15 \text{ \AA}^{-1}$) shows significant deviation from the TB calculated bands. There are strong features forming a “W” shape in the $E(k_{\parallel})$ plot which are not seen in the calculated bands, and structured intensity to lower binding energy than the calculated lowest binding energy band. An equivalent point in the third Brillouin zone ($k_{\perp} = 11.07 \text{ \AA}^{-1}$, photon energy 445 eV) is shown in Fig S1(d), and is a significantly better match for the TB calculations, indicating that TB can replicate the shape of the bands at this point in the zone with reasonable accuracy.

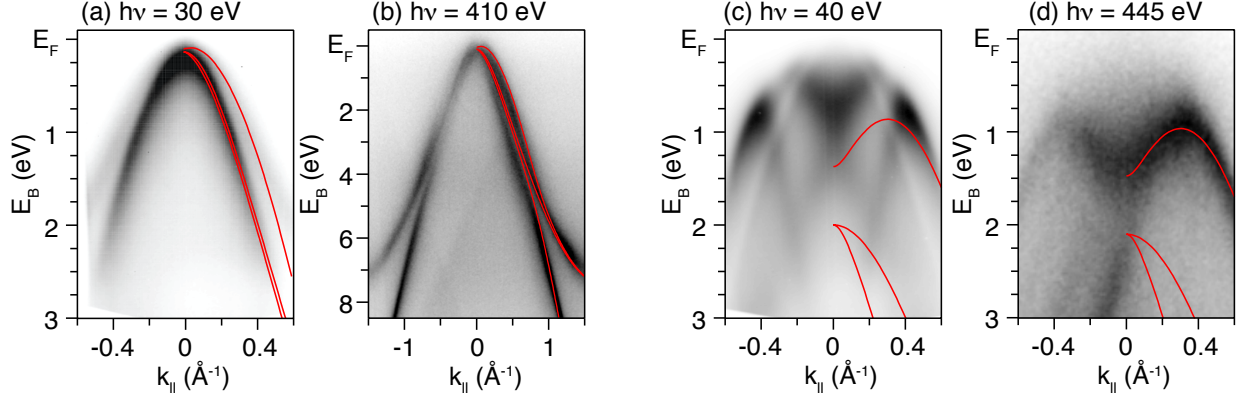


FIG. S1. A demonstration of deviation from free-electron-like final state model in ARPES. (a) The data acquired with a photon energy of 30 eV on a δ -layer sample, and (b) the same measurement performed with 410 eV. Using the assumption of a free-electron-like final state, both of these acquisitions correspond to sampling the plane containing the bulk Γ point (in good agreement with the TB calculations, overlaid in red). Panel (c) shows data acquired with a photon energy of 40 eV, and (d) shows data acquired with 445 eV. Using the assumption of a free-electron-like final state, both acquisitions should correspond to the same position in the bulk Brillouin Zone (partway between Γ and X). At high photon energy, this assumption holds and the data is in good agreement with the overlaid TB calculations (red), but for the $h\nu=40$ eV acquisition, this assumption fails and a broad range of bulk states are seen.

We believe that these unexpected features and behaviour can be explained by the free electron final state (FEFS) model being a poor representation of the low energy final state spectrum in diamond. The FEFS model assumes the only photoemission transitions are direct “vertical” transitions (i.e. the photoelectron momentum \mathbf{k} is the same in the initial and final state), and that the photoexcited electron is promoted into a free-electron plane wave state within a single continuum band. This model is frequently used for interpreting ARPES datasets,[4, 6, 7] and when it applies, ARPES can be understood as a direct measure of the initial state bandstructure. This facilitates a straightforward comparison between experimental data and initial state bandstructures from TB calculations, the $\mathbf{k} \cdot \mathbf{p}$ method

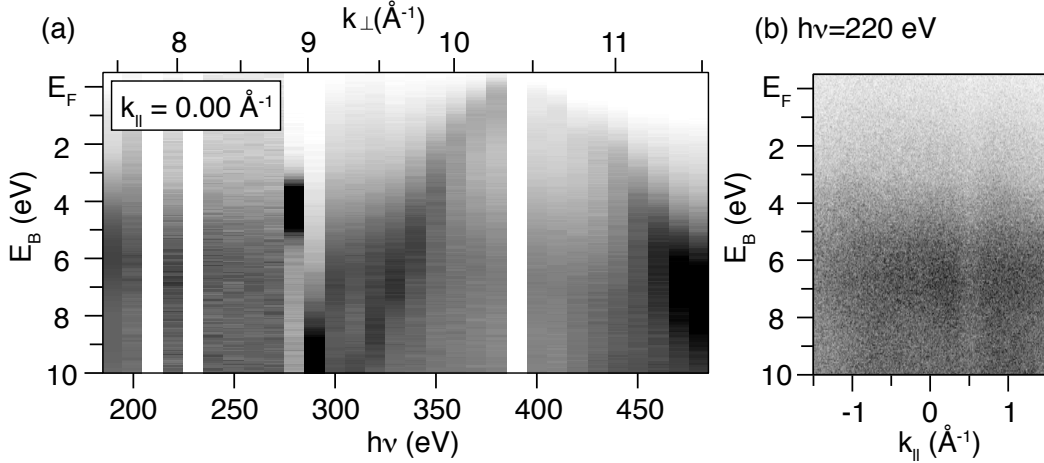


FIG. S2. A demonstration of the issues encountered in performing and interpreting ARPES measurements on diamond with low photon energy. (a) a constant k_{\parallel} slice for measurements performed on the bulk film with photon energies between 190 eV and 480 eV in 10 eV steps (excluding 210 eV, 230 eV and 390 eV) and (b) the 220 eV $E(k_{\parallel})$ plot from this data series.

and Density Functional Theory (DFT). However, the free-electron final state is not always a reasonable assumption for the complete final state distribution in all materials; there may be band gaps, and non free-electron dispersion. Band gaps prevent particular transitions and result in no observed intensity for measurements at particular photon energies, such as we see between 190 eV and 280 eV. Where the final state has non free-electron-like dispersion, additional features may be observed which do not appear in an initial state calculation, such as we see in Fig S1(c) for 40 eV measurements. With increasing photon energy it is expected that the final state distribution should approach a free-electron like continuum at higher energies for all materials, [8, 9] improving the agreement between measured ARPES data and initial state calculations, as we see in Fig S1(d) for 445 eV. Himpsel *et al.* showed that the FEFS model does not apply well to measurements performed on diamond with photon energies less than 100 eV,[5], and our observations suggest that this extends up to a photon energy of approximately 300 eV, after which the agreement between calculations and experimental data suggest that the FEFS model applies until at least 460 eV.

While we find no explicit mention of non-FEFS behaviour between 100 eV and 300 eV for measurements on diamond in the literature, we note that this explains some observations made in a recent study by Guyot *et al.*[10] ARPES measurement are performed with photon

energies below 200 eV and above 350 eV to evaluate the Luttinger parameters for metallic diamond, and observed that measurements conducted with low photon energy (170 eV being a specific energy mentioned by Guyot *et al.*), additional bands appeared. Guyot *et al.* state that these bands could not be replicated with $\mathbf{k} \cdot \mathbf{p}$ bandstructure calculations. As described above, agreement between initial state bandstructure calculations, such as $\mathbf{k} \cdot \mathbf{p}$ calculations, and experimental data relies on the assumption of a free-electron final state. It is clear from the data presented by Guyot *et al.* that there must be some states available for photon energies lower than 190 eV, but given the intensity gap at 200 eV we have inferred from our work, it is unlikely that the final state spectrum at 170 eV is free-electron-like. This likewise gives some explanation for why the $\mathbf{k} \cdot \mathbf{p}$ model employed by Guyot *et al.* predicts bands where none are observed in the low energy data, while matching well with high energy data.

However, it is unclear why the inner potential assessed from measurements performed within the non-FEFS regime appear reasonable. The ARPES studies of Guyot *et al.* and Edmonds *et al.* calculate inner potentials of 17.7 eV and 22 eV respectively, using measurements performed with photon energies below 200 eV, which we could expect would be influenced by the non-free-electron nature of the final state. These values straddle the 18.2 eV found by Ashenford and Lisgarten[11] using the Shinohara method, which is not influenced by the photoelectron final state. This similarity suggests that at some points in the Brillouin zone, such as bulk Γ , the transition into the final state does not differ too significantly from a FEFS transition. This explains the agreement between our TB calculations and the data recorded at 30 eV, near Γ_{001} , while the data acquired at 40 eV deviates significantly from calculations.

III. CONFINEMENT POTENTIAL

In this work, we have stated that our δ -layer has a nominal thickness of 1.8 nm, and the SIMS measurements in the main document confirms that it has FWHM ≤ 4 nm. However, the SIMS measurement presented is limited by the resolution of the instrument, and hence there is some uncertainty in the actual width. This in turn leads to an uncertainty in the expected confinement potential, and therefore in the prediction of occupied quantised states.

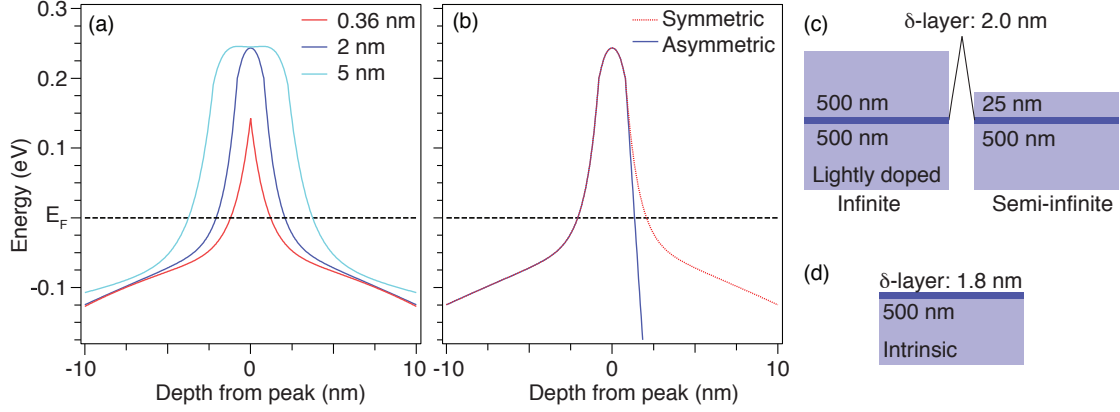


FIG. S3. Sketch of (a) the potentials generated by a thin and thicker δ -layer, (b) a comparison of symmetric and asymmetric δ layer potentials due to the presence and absence of a capping layer, (c) the simulation conditions of Chicot *et al.* and Fiori *et al.* (d) The sample used in this work.

As shown by Chicot *et al.* [12] reducing the thickness of the δ -layer leads to a shallower and narrower potential; this is schematically shown in Fig. S3(a), and more detail may be seen by comparing Figure 1(b) - (d) of Chicot *et al.* [12] A narrower and shallower potential will naturally change the distribution of energy states in the well, and may create a situation where there are no longer occupied quantum well states and, thus, we would expect to see no states in ARPES. On the other hand, the sharpness of the δ -layer needs to be significantly underestimated in order for this to be the case.

Another possible cause for discrepancy is the symmetry of the potential well. Chicot *et al.* and Fiori *et al.* have performed Poisson-Schrödinger calculations of 2 nm δ -layers sandwiched between two 500 nm slabs of diamond (the “infinite” case), while Fiori *et al.* also considers an asymmetric system containing a δ -layer sandwiched between a 500 nm diamond slab and a 25 nm diamond layer with a Schottky contact (the “semi-infinite” case). A schematic diagram of these systems, as well as the non-encapsulated sample used in this experiment, are shown in Fig. S3(c) and (d). Fiori *et al.* show that altering one side of the potential well causes the confined states to shift in energy relative to the Fermi level, as would be expected from simple analytical calculations of a triangular potential. If the potential across the diamond/vacuum interface is significantly steeper than the potential within the diamond, as depicted schematically in Fig. S3(b), this will cause electron-occupied states to shift further

below the Fermi level relative to the symmetric well case. However, the difference in the shape of the confinement potential is not large, and hence we don't believe that this is a feasible explanation for the lack of confined states in our ARPES investigation.

-
- [1] J. E. Butler, A. Vikharev, A. Gorbachev, M. Lobaev, A. Muchnikov, D. Radischev, V. Isaev, V. Chernov, S. Bogdanov, M. Drozdov, E. Demidov, E. Surovegina, V. Shashkin, A. Davydov, H. Tan, L. Meshi, A. C. Pakpour-Tabrizi, M.-L. Hicks, and R. B. Jackman, *Physica Status Solidi (RRL) –Rapid Research Letters* **11**, 1600329 (2017).
 - [2] R. S. Balmer, I. Friel, S. Hepplestone, J. Isberg, M. J. Uren, M. L. Markham, N. L. Palmer, J. Pilkington, P. Huggett, S. Majdi, and R. Lang, *Journal of Applied Physics* **113**, 033702 (2013).
 - [3] J. J. Yeh and I. Lindau, *Atomic Data and Nuclear Data Tables* **32**, 1 (1985).
 - [4] A. Damascelli, *Physica Scripta* **T109** (2004).
 - [5] F. J. Himpsel, J. F. van der Veen, and D. E. Eastman, *Phys. Rev. B* **22**, 1967 (1980).
 - [6] D. Liebowitz and N. J. Shevchik, *Phys. Rev. B* **17**, 3825 (1978).
 - [7] F. J. Himpsel, *Appl. Opt.* **19**, 3964 (1980).
 - [8] A. X. Gray, C. Papp, S. Ueda, B. Balke, Y. Yamashita, L. Plucinski, J. Minár, J. Braun, E. R. Ylvisaker, C. M. Schneider, W. E. Pickett, H. Ebert, K. Kobayashi, and C. S. Fadley, *Nature Materials* **10**, 759 EP (2011).
 - [9] A. Bianconi, S. B. M. Hagström, and R. Z. Bachrach, *Phys. Rev. B* **16**, 5543 (1977).
 - [10] H. Guyot, P. Achatz, A. Nicolaou, P. Le Fèvre, F. Bertran, A. Taleb-Ibrahimi, and E. Bustarret, *Phys. Rev. B* **92**, 045135 (2015).
 - [11] D. E. Ashenford and N. D. Lisgarten, *Acta Crystallographica Section A* **39**, 311 (1983).
 - [12] G. Chicot, A. Fiori, P. N. Volpe, T. N. Tran Thi, J. C. Gerbedoen, J. Bousquet, M. P. Alegre, J. C. Piñero, D. Araújo, F. Jomard, A. Soltani, J. C. De Jaeger, J. Morse, J. Härtwig, N. Tranchant, C. Mer-Calfati, J. C. Arnault, J. Delahaye, T. Grenet, D. Eon, F. Omnès, J. Pernot, and E. Bustarret, *Journal of Applied Physics* **116**, 083702 (2014).